A&A 465, 1–8 (2007)
DOI: 10.1051/0004-6361:20066080

Astronomy & Astrophysics

The low-luminosity tail of the GRB distribution: the case of GRB 980425

F. Daigne and R. Mochkovitch

Institut d'Astrophysique de Paris, UMR 7095 CNRS – Université Pierre et Marie Curie – Paris 6, 98 bis boulevard Arago, 75014 Paris, France e-mail: daigne@iap.fr

Received 21 July 2006 / Accepted 23 November 2006

ABSTRACT

Context. The association of GRB 980425 with the nearby supernova SN 1998bw at $z = 0.0085$ implies the existence of a population of gamma-ray bursts with an isotropic-equivalent luminosity that is about 10^4 times lower than in the standard cosmological case. Apart from its weak luminosity, GRB 980425 appears a "normal" burst based on all its other properties (variability, duration, spectrum), with however a rather low peak energy of $E_p \simeq 30-100$ keV.

Aims. We investigate two scenarios to explain a weak gamma-ray burst such as GRB 980425: a normal (intrinsically bright) gamma-ray burst seen off-axis or an intrinsically weak gamma-ray burst seen on-axis.

Methods. For each of these two scenarios, we first derive the conditions to produce a GRB 980425-like event and then discuss the consequences for the event rate. In the second scenario, this study is done in the framework of the internal shock model.

Results. If we exclude the possibility that GRB 980425 is an occurrence of an extremely rare event observed by chance during the first eight years of the "afterglow era", the first scenario implies that (i) the local rate of "standard" bright gamma-ray bursts is much higher than what is usually expected; and (ii) the typical opening angle in gamma-ray bursts ejecta is much narrower than what is derived from observations of a break in the afterglow lightcurve. In addition to this statistical problem, we show that the afterglow of GRB 980425 in this scenario should have been very bright and easily detected. For these reasons the second scenario appears more realistic. We show that the parameter space of the internal shock model indeed allows GRB 980425-like events, in cases where the outflow is only mildly relativistic and mildly energetic. The rate of such weak events in the Universe has to be much higher than the rate of "standard" bright gamma-ray bursts to allow the discovery of GRB 980425 during a short period of a few years. However, it is still compatible with the observations, as the intrinsic weakness of these GRB 980425-like bursts does not allow detection at cosmological redshift with present gamma-ray instruments. We briefly discuss the consequences of such a high local rate of GRB 980425-like events for the future prospects of detecting non-electromagnetic radiation, especially gravitational waves.

Key words. gamma rays: bursts – star: supernovae: individual: SN1998bw – shock waves – radiation mechanisms: non-thermal

1. Introduction

Our knowledge of the gamma-ray burst (GRB) population has dramatically increased in the recent years. In addition to "standard" cosmological, bright GRBs peaking at 100 keV−1 MeV, several classes of parent objects have been discovered: X-ray Flashes (XRFs) and X-ray Rich GRBs (XRRs) that peak at much lower energy (Heise et al. 2001; Kippen et al. 2001; Barraud et al. 2003), weak GRBs (such as GRB 031203, Sazonov et al. 2004; Soderberg et al. 2004) and even a few "local" events: GRB 980425 (Galama et al. 1998) and GRB 060218 (Mirabal et al. 2006). It is usually believed that a long GRB is produced by an ultra-relativistic outflow ejected from a black hole that has just formed in the collapse of a very massive star (collapsars, Woosley 1993). The prompt GRB emission originates from the relativistic ejecta itself, and is probably due to the formation of internal shocks (Rees & Meszaros 1994), whereas the afterglow is emitted by the strong shock that propagates within the ambient medium during the deceleration phase of the outflow (Meszaros & Rees 1997).

It is important to understand the physical origin of the observed diversity in this theoretical framework. There are two groups of explanations. Either the diversity is only apparent, where all GRBs are intrinsically very similar but the observation conditions (viewing angle, for instance) break this similarity, or the diversity is intrinsic, meaning all collapsars produce neither the same relativistic outflow nor the same GRB.

In this paper, we focus on the closest GRB, i.e. GRB 980425. This burst has been detected by *Beppo-SAX* and *BATSE*. It is a single-pulse burst with the following gamma-ray properties: duration $T_\gamma \sim 31$ s, peak flux (40−700 keV) $P \sim 2.4 \times 10^{-7}$ erg/cm^2/s, a spectrum reproduced well by the phenomenological Band spectrum (Band et al. 1993) with low- and high-energy slopes $\alpha \sim -0.8$ and $\beta \sim -2.3$, and peak energy $E_p \sim 68 \pm 40$ keV (Frontera et al. 2000). With perhaps the exception of a somewhat lower peak energy (see, however, Ghisellini et al. 2006), all these properties are very close to those of standard GRBs. Note also that Norris et al. (2000) derived an especially large time lag for this burst between *BATSE* channels 1 and 3: $\Delta t_{13} \sim 4.5$ s (typical values for long bursts are $\Delta t_{13} \lesssim 0.1$ s).

A peculiar type Ic supernova, SN 1998bw, was discovered simultaneously in the *Beppo-SAX* error-box (Galama et al. 1998). The probability of having two such rare events occur at the same time in the same direction is very low, so that GRB 980425 and SN 1998bw are probably physically associated (see also Kouveliotou et al. 2004). This is reinforced by other associations that have been found since 1998, the best case probably being

the association of GRB 030329 with SN2003dh (Stanek et al. 2003) at $z = 0.168$. If the association GRB 980425/SN 1998bw is real, then this burst is far from "standard". The host galaxy of SN 1998bw is indeed located at $z = 0.0085$, and GRB 980425 is therefore the closest GRB ever detected. As the peak flux of GRB 980425 is comparable to typical peak fluxes of other *Beppo-SAX* GRBs, it means that it is intrinsically much weaker (by more than four orders of magnitude).

In Sect. 2, we recall the various physical factors entering in the observed peak flux and peak energy of a cosmic GRB. We then study a scenario in Sect. 3 where GRB 980425 is a standard bright GRB seen off-axis and, therefore apparently weak. In Sect. 4 we give an alternative explanation where GRB 980425 is intrinsically weak and show how the internal shock model can allow for such weak bursts. In both Sects. 3 and 4 we discuss the consequences of each scenario in terms of the GRB rate. Our results are summarized in Sect. 5.

2. Peak flux and peak energy of a cosmic GRB

We assume that a GRB is produced by a relativistic outflow of Lorentz factor Γ and opening angle $\Delta\theta \gg 1/\Gamma$ generated by a source at redshift z (see Fig. 1). We define θ_0 as the angle between the line-of-sight and the axis of the ejecta. The observed bolometric peak flux and peak energy are given by

$$P^{\rm obs} = \mathcal{K}_{\rm P}\left(\Gamma;\Delta\theta;\theta_0\right) \times \frac{L_{\rm rad,4\pi}}{4\pi D_{\rm L}^2} \tag{1}$$

and

$$E_p^{\rm obs} = \mathcal{K}_{\rm E}\left(\Gamma;\Delta\theta;\theta_0\right) \times \frac{E_{\rm p}}{1+z}, \tag{2}$$

where $L_{\rm rad,4\pi}$ and $E_{\rm p}$ are the isotropic equivalent luminosity and the peak energy measured in the GRB source frame. The corrections for the viewing angle are approximatively given in the on-axis and the off-axis cases by

$$\mathcal{K}_{\rm P}\left(\Gamma;\Delta\theta;\theta_0\right) = \begin{cases} 1 & \text{if } \theta_0 < \Delta\theta \\ \frac{1}{2\left(1+\Gamma^2(\theta_0-\Delta\theta)^2\right)^3} & \text{if } \theta_0 > \Delta\theta \end{cases} \tag{3}$$

and

$$\mathcal{K}_{\rm E}\left(\Gamma;\Delta\theta;\theta_0\right) = \begin{cases} 1 & \text{if } \theta_0 < \Delta\theta \\ \frac{1}{1+\Gamma^2(\theta_0-\Delta\theta)^2} & \text{if } \theta_0 > \Delta\theta. \end{cases} \tag{4}$$

These two approximate expressions of the correction for the viewing angle are derived from the exact formulae that can be found in Granot et al. (1999) and Woods & Loeb (1999). From Eqs. (3) and (4), the peculiar properties of GRB 980425 may have two origins: (i) either GRB 980425 is a "standard" GRB, i.e. intrinsically bright with $L_{\rm rad,\,4\pi} \gtrsim$ a few 10^{50} erg s^{-1}, but appears as a weak GRB because it is seen with a large viewing angle; (ii) or GRB 980425 is an intrinsically weak GRB ($L_{\rm rad,\,4\pi} \simeq 3\times10^{46}$ erg s^{-1}) seen on-axis. In this case GRB 980425 has been detected only because of its very low redshift. In the following, we successively investigate these two scenarios. The first one has already been addressed by several authors (e.g. Nakamura 1999; Salmonson 2001; Yamazaki et al. 2003; Guetta et al. 2004), so we focus mainly on the second scenario. For this case, the intrinsic properties of GRBs are studied in the framework of the internal shock model, where the prompt emission comes from a relativistic wind that converts part of its kinetic energy into radiation via the formation of shock waves within the wind itself. Such internal shocks can occur if the wind is generated with a highly variable Lorentz factor (Rees & Meszaros 1994).

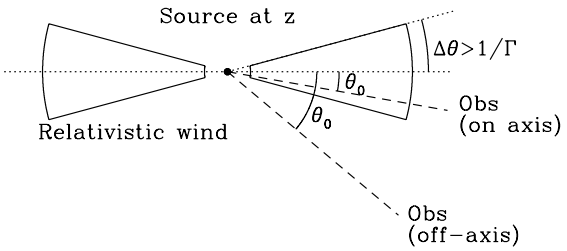

Fig. 1. Geometry. A relativistic outflow of Lorentz factor Γ is emitted by the source (located at redshift z) in a cone of opening angle $\Delta\theta$. The line-of-sight of the observer makes an angle θ_0 with the axis of the cone. The observation is made on-axis (resp. off-axis) if $\theta_0 \leq \Delta\theta$ (resp. $\theta_0 > \Delta\theta$).

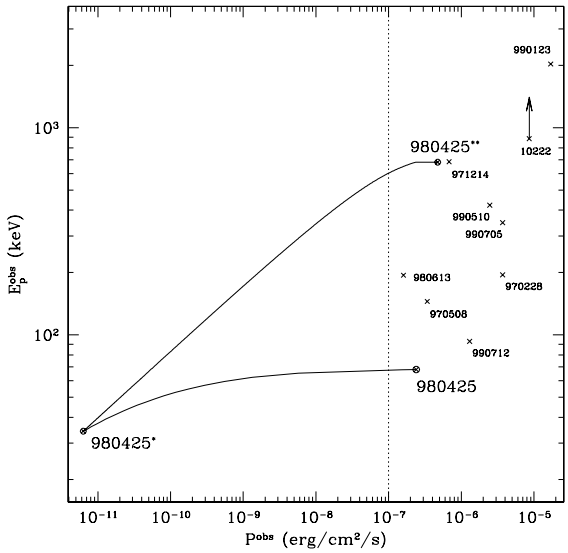

Fig. 2. Bolometric peak flux vs. peak energy diagram: All *Beppo-SAX* GRBs with a known redshift are indicated in this diagram (crosses). The peculiar burst GRB 980425 is indicated by a circled cross. A vertical dotted line stands for a threshold $P_{\rm min} = 10^{-7}$ erg cm^{-2} s^{-1} representative of the *BATSE* and *Beppo-SAX WFC+GRBM* instruments (Band 2003). *Effect of the redshift:* we plotted the evolution of GRB 980425 when its redshift increases from $z = 0.008$ to $z = 1$ (cosmological distance). The final result is indicated as GRB 980425*. *Effect of the viewing angle:* we then plotted the evolution of GRB 980425* when the viewing angle decreases. We assume that GRB 980425* is seen off-axis with $\theta_0 = \Delta\theta + 4/\Gamma$ (see text). The final result for $\theta_0 = 0$ (on-axis) is indicated as GRB 980425**.

3. GRB 980425 as an intrinsically bright GRB seen off-axis

In this section, we first describe how a large viewing angle can account for the observed properties of GRB 980425. We then explain why this scenario suffers a statistical problem, the expected rate of GRB 980425-like events being very low.

3.1. Conjugate effect of a low redshift and a large viewing angle

In Fig. 2, GRB 980425 has been plotted in a bolometric peak flux vs. peak energy diagram, together with the GRBs detected by *Beppo-SAX*, which have a known redshift. A sensitivity of 10^{-7} erg cm^{-2} s^{-1} representative of the *BATSE* and *Beppo-SAX GRBM+WFC* instruments is also indicated (Band 2003). We use Eqs. (1)–(4) to estimate under which conditions on the redshift and the viewing angle GRB 980425 can be an

intrinsically bright GRB despite its low apparent intensity. To clarify the respective roles of redshift and viewing angle, we perform the following two transformations:

- *Effect of the redshift*: GRB 980425 has first been moved from $z = 0.008$ to $z = 1$ (cosmological distance). Both the peak energy and the peak flux decrease due to the increase in redshift and luminosity distance. The final result is named GRB 980425*: this burst is clearly much too weak to be observed as a GRB or even a XRF. Its bolometric peak flux is indeed at least three orders of magnitude below the sensitivity of past or current detectors.
- *Effect of the viewing angle* : the viewing angle of GRB 980425* is then decreased down to $\theta_0 = 0$ (on-axis observation), assuming that GRB 980425 is initially seen off-axis with a large viewing angle $\theta_0 = \Delta\theta + k/\Gamma$ (here $k = 4$). This evolution is computed from the approximate formulae (3) and (4). The final result is named GRB 980425**, and this burst is now clearly back in the "standard" GRB region, very close to GRB 971214. As already pointed out by Yamazaki et al. (2003), the peculiar properties of GRB 980425 are compatible with those of an intrinsically bright GRB observed off-axis. In the case illustrated in Fig. 2, the decrease in the flux of GRB 980425 by a factor $\sim 10^4$ due to a viewing angle $\theta_0 = \Delta\theta + 4/\Gamma$ is compensated by a smaller luminosity distance $(D_{\rm L}(z = 0.008)/D_{\rm L}(z = 1))^2 \sim 2 \times 10^{-4}$.

If it is clear from the previous analysis that a slightly off-axis viewing angle ($\theta_0 - \Delta\theta \sim 4/\Gamma \sim 2.3^\circ$ if $\Gamma \simeq 100$) can account for the properties of GRB 980425, one should however keep in mind that the peak flux decreases very rapidly with viewing angle (see Eq. (3)). For $\theta_0 = \Delta\theta + k/\Gamma$ with $k \geq 6$, the peak flux is divided by a factor larger than $\sim 10^5$ and the decrease in luminosity distance is no longer able to compensate: such off-axis GRBs cannot be detected. As $\Gamma \gtrsim 100$ in GRB outflows (Baring 1995; Lithwick & Sari 2001), the angle $6/\Gamma \lesssim 3.4^\circ$ is small and the probability of observing GRB 980425-like events should be low.

3.2. A statistical problem?

For a detector with a threshold $P_{\rm min}$ (hereafter we assume $P_{\rm min} = 10^{-7}$ erg cm^{-2} s^{-1}, which is representative of instruments such as *Beppo-SAX GRBM+WFC* or *BATSE*), the observed rate of on-axis GRBs within $D = 40$ Mpc is given by

$$\mathcal{R}_{\rm on} = \frac{4\pi}{3} D^3 R_0 \times \int_0^{\pi/2} {\rm d}\Delta\theta \; p\,(\Delta\theta)\,(1 - \cos\Delta\theta)\,, \qquad (5)$$

where R_0 is the local GRB volumic rate and $p(\Delta\theta)$ the probability distribution of the opening angle $\Delta\theta$. Here we assume that the minimum GRB luminosity $L_{\rm min}$ is higher than $4\pi D^2 P_{\rm min} = 2\times 10^{46}$ erg s^{-1}, so that all nearby on-axis GRBs are detected. On the other hand, the rate of off-axis GRBs in the same volume is affected by the rapid decrease in the GRB flux with the opening angle so that

$$\mathcal{R}_{\rm off} = R_0 \int_0^D {\rm d}D\, 4\pi D^2 \int_0^{\pi/2} {\rm d}\Delta\theta\; p\,(\Delta\theta) \int_{L_{\rm min}}^{L_{\rm max}} {\rm d}L\; p(L) \times \left(\cos\Delta\theta - \cos\left(\Delta\theta + \frac{k_{\rm max}\,(D,L)}{\Gamma}\right)\right), \qquad (6)$$

where $p(L)$ is the GRB luminosity function and $k_{\rm max}$ is given by

$$k_{\rm max}\,(D,L) \simeq \sqrt{\left(\frac{1}{2}\,\frac{L}{4\pi D^2 P_{\rm min}}\right)^{1/3} - 1}. \qquad (7)$$

In both Eqs. (6) and (7), the probability distribution of the Lorentz factor Γ is neglected and Γ is supposed to be constant. In the simplest case where both the luminosity L and the opening angle $\Delta\theta$ are constant, we find that the ratio of detected off-axis over on-axis GRBs can be expressed as a ratio of two solid angles:

$$\frac{\mathcal{R}_{\rm off}}{\mathcal{R}_{\rm on}} \simeq \frac{\cos\Delta\theta - \cos\left(\Delta\theta + \frac{k_{\rm max}(D,L)}{\Gamma}\right)}{1 - \cos\Delta\theta}. \qquad (8)$$

For $D = 40$ Mpc and $L = 10^{51}$ erg s^{-1}, we get $k_{\rm max} = 5.4$, so that $k_{\rm max}/\Gamma \lesssim 3.1^\circ$ for $\Gamma \gtrsim 100$. This leads to a rate of detected off-axis over on-axis GRBs $\mathcal{R}_{\rm off}/\mathcal{R}_{\rm on} \sim 16$ for $\Delta\theta = 1^\circ$, $\mathcal{R}_{\rm off}/\mathcal{R}_{\rm on} \sim 1$ for $\Delta\theta = 7.5^\circ$, and $\mathcal{R}_{\rm off}/\mathcal{R}_{\rm on} \sim 0.7$ for $\Delta\theta = 10^\circ$. This implies that the rates of detected off-axis and on-axis GRBs should be comparable for typical $\Delta\theta$ of a few degrees and that it is only for $\Delta\theta \lesssim 1^\circ$ that the number of detected off-axis GRBs is much larger than the number of on-axis GRBs. The local apparent rate of "standard" on-axis bright GRBs can be estimated to be $\sim 1/\,(5000{-}30\,000$ yr) within 40 Mpc (Porciani & Madau 2001; Schmidt 2001; Perna et al. 2003; Guetta et al. 2004). This simple analysis would then imply that, with GRB 980425, we have by chance observed a very rare event. Even if it has some rather different properties, GRB 060218/SN2006aj at $z = 0.0331$ (144 Mpc) (Cusumano et al. 2006; Mirabal et al. 2006; Masetti et al. 2006; Soderberg et al. 2006a) is another case of a nearby burst. At this distance $\mathcal{R}_{\rm off}/\mathcal{R}_{\rm on}$ should be even smaller. Statistical studies (Bosnjak et al. 2006) also indicate that there are probably other GRB980425-like events in the *BATSE* catalog. For all these reasons, we conclude that the off-axis interpretation suffers a statistical problem.

In the more general case, the two solid angles in Eq. (8) have to be averaged over the luminosity function, the distance and the opening angle distribution, according to Eqs. (6) and (7). We did that for a power-law luminosity function with slope -1.7 (this slope giving a good fit to the $\log N - \log P$ diagram, see e.g. Daigne et al. 2006) between $L_{\rm min} = 10^{50}$ erg s^{-1} and $L_{\rm max} = 10^{54}$ erg s^{-1}. We tested three possible distributions for the opening angle: (1) a uniformly distributed opening angle; (2) a power-law distributed opening angle; (3) an opening angle correlated with the isotropic equivalent luminosity so that the true luminosity is constant, as suggested by observations of achromatic breaks in afterglow lightcurves (Frail et al. 2001). We find (see Fig. 3) that, except below $\sim$5 Mpc where the total (on+off axis) event rate is very low due to a smaller volume, the expected rate of off-axis GRBs is either comparable (uniformly distributed opening angle) or lower than the on-axis GRB rate. This is in full agreement with our simple estimate (Eq. (8)). This equation also indicates that the only way to have a much higher rate of off-axis GRBs is to assume a very small opening angle ($\Delta\theta \ll 1/\Gamma$), in contradiction with observations (Frail et al. 2001).

The analysis in this section has been done using the so-called "uniform jet" model, i.e. a jet where the Lorentz factor and the energy per unit solid angle is constant within the opening angle $\Delta\theta$. Our results will, however, not be changed if we assume a "universal structured jet" (Rossi et al. 2002) where the Lorentz factor and the energy per unit solid angle have a powerlaw shape within $\Delta\theta$. Indeed the less luminous part of such a structured jet is located at the edge and still corresponds to $L_{\gamma,\,4\pi} \gtrsim 10^{50}$ erg s^{-1}, which means that such a jet is always detected within 40 Mpc when seen with a viewing angle $\theta_0 \leq \Delta\theta$. The estimate of $\mathcal{R}_{\rm on}$ is then unchanged. The estimate of the rate of off-axis detections with $\theta_0 > \Delta\theta$, which would lead to GRB 980425-like events, is also unchanged, assuming

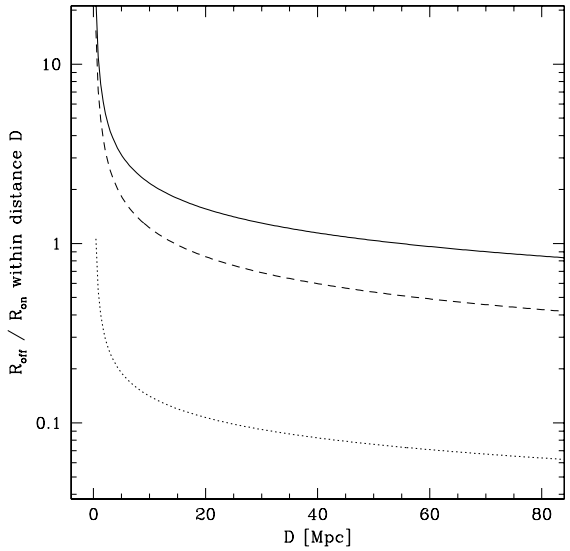

Fig. 3. The ratio of detected off-axis to on-axis GRBs in the local Universe: this ratio within a distance D is plotted as a function of D for a power-law luminosity function of slope -1.7 between $L_{\rm min} = 10^{50}$ erg s^{-1} and $L_{\rm max} = 10^{54}$ erg s^{-1} and three different distributions of the opening angle: (1) a uniformly distributed opening angle between 1 and 10° (solid line); (2) a power-law distribution $p(\Delta\theta) \propto \Delta\theta^{-2}$ between $1/\Gamma$ and $\pi/2$ (dashed line); (3) an opening angle correlated with the isotropic luminosity (dotted line). In this last case, the true luminosity $L\,(1-\cos\Delta\theta)$ is assumed to be constant and equal to $L_{\rm min}$.

the values observed at the edge of the structured jet for L and Γ. Therefore we conclude that, either in the uniform jet model or in the universal structured jet model, the off-axis interpretation of GRB 980425 is not working statistically.

4. GRB 980425 as an intrinsically weak GRB

We now consider in this section an alternative scenario where GRB 980425 is an intrinsically weak GRB seen on-axis. The intrinsic GRB properties are considered in the framework of the internal shock model (Rees & Meszaros 1994).

4.1. Internal shocks

The dynamics of the internal shocks, as well as the temporal and spectral properties of the emission, have been studied in detail in Daigne & Mochkovitch (1998) using a simplified model where the outflow is made of a large number of discrete relativistic shells that interact by direct collisions only. This approach has been validated by 1D relativistic hydrodynamical simulations (Daigne & Mochkovitch 2000). We adopt here an even simpler version of the model, where we consider only a typical internal shock due to the collision of two shells of equal mass M and Lorentz factors Γ_1 and $\Gamma_2 > \Gamma_1$. This toy model is described in Barraud et al. (2005). It is found that the collision between the two shells occurs at radius

$$R_{\rm is} \simeq \frac{8\kappa^2}{(\kappa-1)(\kappa+1)^3}\Gamma^2 c\tau, \tag{9}$$

that the isotropic equivalent radiated luminosity due to internal shocks is given by

$$L_{\rm rad,4\pi} \simeq \epsilon_{\rm e}\frac{(\sqrt{\kappa}-1)^2}{\kappa+1}\dot{E}, \tag{10}$$

and that the peak energy takes the form

$$E_{\rm p} \simeq K\frac{\dot{E}^x\,\phi_{xy}(\kappa)}{\tau^{2x}\,\Gamma^{6x-1}}, \tag{11}$$

where $\dot{E}$ is the isotropic equivalent kinetic energy injection rate in the relativistic outflow, τ the duration of the relativistic ejection (i.e. here the time interval between the two shell ejections), Γ the mean Lorentz factor $(\Gamma_1+\Gamma_2)/2$, and the contrast $\kappa = \Gamma_2/\Gamma_1$ is a measure of the initial amplitude of the variations of the Lorentz factor in the ejecta. Also $\epsilon_{\rm e}$ is the fraction of the dissipated energy in the shock that is injected into non-thermal electrons, and K is a constant. The function $\phi_{xy}(\kappa)$ is given by

$$\phi_{xy}(\kappa) = \frac{\left(\sqrt{\kappa}-1\right)^{2y}(\kappa-1)^{2x}(\kappa+1)^{6x-1}}{\kappa^{2x+\frac{y-1}{2}}} \tag{12}$$

and is steadily increasing with κ. The x and y parameters have been introduced by considering that the peak energy in the comoving frame of the shocked material scales as

$$E'_{\rm p} \propto \rho^x \epsilon^y, \tag{13}$$

where ρ is the comoving density and ϵ the dissipated energy per unit mass.

In the standard synchrotron model with constant equipartition parameters, it is assumed that the magnetic field is amplified to reach a fraction $\epsilon_{\rm B}$ of the total dissipated energy in the shock and that a fraction $\epsilon_{\rm e}$ of this dissipated energy is injected into a fraction ζ of the electrons, which are therefore accelerated to high Lorentz factors. This leads to $x = 1/2$ and $y = 5/2$, as the synchrotron energy scales as $E'_{\rm p} \propto B\Gamma_{\rm e}^2$, the magnetic field as $B \propto \epsilon_{\rm B}^{1/2}(\rho\epsilon)^{1/2}$, and the typical Lorentz factor of the electrons as $\Gamma_{\rm e} \propto (\epsilon_{\rm e}/\zeta)\epsilon$. However, Daigne & Mochkovitch (2003) have shown that lower values of x and y are required to reproduce the hardness-intensity and hardness-fluence correlations observed in many GRB pulses (Golenetskii et al. 1983; Liang & Kargatis 1996). They consider $x = y = 0.5$ and $x = y = 0.25$. Such exponents can, for example, be obtained with the standard synchrotron process if the equipartition parameters vary with shock intensity.

4.2. Producing GRB980425-like events

The value of $L_{\rm rad,4\pi}$ and $E_{\rm p}$ given by Eqs. (10) and (11) are fixed by 6 physical quantities: $\dot{E}$, $\bar{\Gamma}$, κ, τ, $\epsilon_{\rm e}$, and K. The values of $\epsilon_{\rm e}$ and K depend on the details of the physical processes in the shocked material, which are not studied here. We adopt $\epsilon_{\rm e} = 1/3$ and fix the value of K by demanding that a "typical" GRB at redshift $z = 1$ with $\tau = 5$ s (observed duration of $(1+z)\tau = 10$ s), $\kappa = 4$, $\dot{E} = 1.5\times10^{52}$ erg s^{-1} ($L_{\rm rad,4\pi} = 10^{51}$ erg s^{-1}) and $\bar{\Gamma} = 300$ has an observed peak energy $E_{\rm p}^{\rm obs} = 200$ keV. Note that, in this case, the efficiency of internal shocks is $L_{\rm rad,4\pi}/\dot{E} = 6.7\%$, as the product of $\epsilon_{\rm e} = 1/3$ with an internal shock dynamical efficiency of 20% for $\kappa = 4$ (see Eq. (10)). The other parameters are limited by several constraints (Daigne & Mochkovitch 2004).

(1) Transparency during the internal shock phase. The relativistic ejecta has to be transparent during the internal shock phase. The Thomson optical depth of the outflow is given by (Mészáros & Rees 2000; Daigne & Mochkovitch 2002):

$$\tau(R_{\rm is}) \simeq \frac{\sigma_T\dot{E}\tau}{4\pi\Gamma R_{\rm is}\left(R_{\rm is}+2\Gamma^2 c\tau\right)m_{\rm p}c^2}. \tag{14}$$

Then the condition $\tau(R_{\rm is}) < 1$ leads to

$$\frac{\dot{E}}{\Gamma^5} < \frac{4\pi m_{\rm p} c^4}{\sigma_{\rm T}} f_1(\kappa)\, \tau, \tag{15}$$

with

$$f_1(\kappa) = \frac{8\kappa^2}{(\kappa-1)(\kappa+1)^3}\left(\frac{8\kappa^2}{(\kappa-1)(\kappa+1)^3}+2\right). \tag{16}$$

(2) No pair production. The relativistic ejecta has to be transparent to pairs during the internal shock phase. Pairs are produced by photon-photon annihilation in the high-energy part of the GRB spectrum. At radius $R_{\rm is}$, the approximate optical depth for pair creation is (Mészáros & Rees 2000; Lithwick & Sari 2001):

$$\tau_{\pm}(R_{\rm is}) \simeq \left[\alpha_{\pm}\frac{\sigma_{\rm T} L_{\rm rad,4\pi}\tau}{4\pi R^2 \Gamma m_{\rm e} c^2}\left(\frac{E_{\rm p}}{\Gamma m_{\rm e} c^2}\right)^{\beta-2}\right]^2, \tag{17}$$

where β is the high-energy slope of the spectrum and $\alpha_{\pm}$ is a dimensionless number that depends on the spectral shape. In the following, we adopt $\beta = 2.5$ (Preece et al. 2000). This leads to $\alpha_{\pm} \simeq 0.06$. Then the condition $\tau_{\pm}(R_{\rm is}) < 1$ leads to

$$\frac{\dot{E}^{1+x(\beta-2)}}{\Gamma^{5+6x(\beta-2)}} < \frac{4\pi m_{\rm e} c^4}{\alpha_{\pm}\sigma_{\rm T}}\frac{f_2(\kappa)}{\epsilon_{\rm e}}\left(\frac{K}{m_{\rm e}c^2}\right)^{2-\beta}\tau^{1+2x(\beta-2)} \tag{18}$$

with

$$f_2(\kappa) = \frac{64\kappa^4}{(\sqrt{\kappa}-1)^2(\kappa-1)^2(\kappa+1)^5\,\Phi_{xy}^{\beta-2}(\kappa)}. \tag{19}$$

We also considered an additional constraint provided by the lack of an observed high-energy cutoff due to photon-photon annihilation in GRB spectra (see e.g. Lithwick & Sari 2001). However, the constraint expressed by Eq. (18) is dominant in most cases.

(3) Internal shocks operate before the deceleration phase. The internal shock phase has to occur before the deceleration of the ejecta due to the external medium. For a density $\rho \propto A/R^s$ in the environment, the deceleration starts at

$$R_{\rm dec} \simeq \left(\frac{3-s}{4\pi}\,\frac{\dot{E}\tau}{A\Gamma^2 c^2}\right)^{\frac{1}{3-s}}. \tag{20}$$

Then the condition $R_{\rm is} < R_{\rm dec}$ leads to

$$\frac{\dot{E}}{\Gamma^{8-2s}} > \frac{4\pi}{3-s} A c^{5-s}\tau^{2-s}\left(\frac{8\kappa^2}{(\kappa-1)(\kappa+1)^3}\right)^{3-s}. \tag{21}$$

Figure 4 shows the location of these constraints, as well as lines of constant peak energy in the Γ–$\dot{E}$ plane for two sets of the x and y parameters: $x = y = 1/4$ (top) and $x = y = 1/2$ (bottom) and for two possible environments: either a uniform medium ($s = 0$) with $n = A/m_{\rm p} = 1$ cm^{-3} (left column) or a dense stellar wind ($s = 2$) with $A_* = A/\left(5\times10^{11}\ {\rm g\ cm^{-1}}\right) = 0.1$ (right column). The other parameters are fixed: $\tau = 30$ s, which is the duration of GRB 980425, and $\kappa = 4$. The transparency constraint is dominated by Eq. (18) (optical depth for pair creation) and not by Eq. (15) (Thomson opacity of ambient electrons). The environment constraint (Eq. (21)) is much stronger in the case of a stellar wind. For winds denser than $A_* = 0.1$ (WR stars may have $A_* \gtrsim 1$), it becomes very difficult for internal shocks to operate before deceleration starts. This problem was already mentioned in Daigne & Mochkovitch (1999, 2001).

Despite these constraints, the internal shock model can explain a wide range of bolometric luminosities and peak energies, in agreement with the observed GRB diversity. As can be seen in Fig. 4, the internal shock model allows the existence of GRB980425-like events at $z = 0.0085$, except in the case of a wind environment with $x = y = 1/2$. These weak GRBs correspond to mildly relativistic ($\Gamma \simeq 10-20$) and mildly energetic ($\dot{E} \simeq 5\times10^{47}$ erg s^{-1}) outflows. On the other hand, Fig. 5 confirms that at cosmological distance ($z = 1$), only "standard" GRBs with highly relativistic ($\Gamma \gtrsim 30$) and highly energetic ($\dot{E} \gtrsim 10^{51}$ erg s^{-1} can be detected. Notice that Fig. 5 show no XRFs or XRRs, i.e. no GRBs with low peak energies ($E_{\rm p} \lesssim 50$ keV). As explained in Barraud et al. (2005), these soft GRBs are produced in outflows with high Lorentz factors Γ and low contrasts κ, i.e. outflows with a very low baryonic pollution and a smoother ejection. This is illustrated in Fig. 6 where the effect of a low constrast κ is shown.

4.3. The afterglow of GRB 980425-like events

The afterglow of a "standard" GRB at 40 Mpc should be $\sim 10 = 5\log\left(D(z\sim1)/40\ {\rm Mpc}\right)$ magnitudes brighter than for a cosmological GRB, due to the short distance. It would then easily peak at the fifth magnitude in V band. Such a bright afterglow was not detected in association with GRB 980425. The emission in V band is entirely dominated by the lightcurve of SN1998bw (Galama et al. 1998) (see bottom panel of Fig. 7), and no afterglow was detected. In X-ray, the WXM of *Beppo-SAX* has detected a weak decreasing source that could be the X-ray afterglow: see the filled circles in the top panel of Fig. 7 (Pian et al. 2000). Note that only the first point is a firm detection. Any scenario for GRB 980425 should then predict a weak afterglow to be consistent with these data.

We have plotted in Fig. 7 the predicted lightcurve in X-rays and in the V band of the afterglow for each of the two scenarios considered in this paper. Again, the external medium is either a stellar wind with $s = 2$ and $A_* = 0.1$ or a uniform medium with $s = 0$ and $n = 1$ cm^{-3}. The first case (wind environment) should be preferred due to the association of GRB 980425 with SN1998bw. The afterglow is computed assuming "typical" values for the parameters: $p = 2.5$ (slope of the electron power law distribution), $\epsilon_{\rm e} = 0.1$ (fraction of dissipated energy injected in relativistic electrons), and $\epsilon_{\rm B} = 10^{-3}$ (fraction of dissipated energy injected in magnetic field). In the case of an intrinsically weak GRB seen on-axis, we have adopted $\Gamma_0 = 10$ for the initial Lorentz factor and $E_0 = 6\times10^{48}$ erg for the initial kinetic energy, according to our analysis of the prompt emission. The initial Lorentz factor and kinetic energy in the case of an intrinsically bright GRB seen off-axis have "standard" values $\Gamma_0 = 100$ and $E_0 = 10^{53}$ erg. The opening angle is fixed to $\Delta\theta = 5°$ and the viewing angle to $\theta_0 = \Delta\theta + 4/\Gamma_0$ (see Sect. 3).

It clearly appears that the predicted afterglow is much too bright in the off-axis scenario. It should have been easily detected in X-rays or in the V band. This is again evidence against the off-axis scenario (Waxman 2004a,b). A discussion based on the radio afterglow leads to the same conclusion (Waxman 2004b; Soderberg et al. 2006a). To decrease the afterglow flux, one should either consider a very low density environment: $A_* \lesssim 3\times10^{-4}$ ($s = 2$) or $n \lesssim 10^{-5}$ cm^{-3} ($s = 0$) or assume very low equipartition parameters such as $\epsilon_{\rm e} < 5\times10^{-4}$ or $\epsilon_{\rm B} < 10^{-7}$. On the other hand, the afterglow is very weak in the case of an intrinsically weak GRB seen on-axis, due to the low value of the

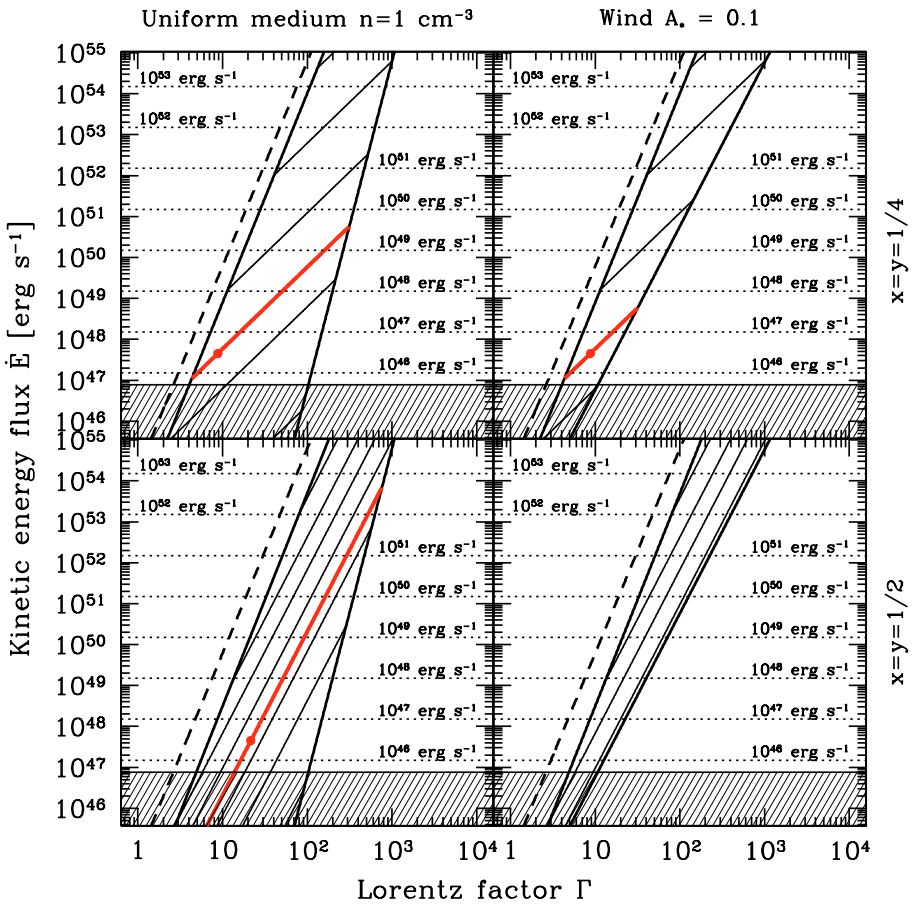

Fig. 4. The internal shock model parameter space at $z = 0.0085$. In the Γ–$\dot{E}$ plane, lines of constant peak energy (observer frame) are plotted for $\kappa = 4$, $\tau = 30$ s, $\epsilon_e = 1/3$, and a fixed value of K computed as explained in the text. These lines are limited on the left side by the transparency constraint given by Eq. (18) (optical depth for pair creation: solid line) and (15) (opacity due to ambient electrons: dashed line) and on the right side by the environment constraint given by Eq. (21). As κ and ϵ_e are fixed, the radiative efficiency is also fixed to 6.7% (see text): thin dotted horizontal lines show the radiated luminosity $L_{\rm rad,4\pi}$ corresponding to the injected kinetic energy rate $\dot{E}$. The shaded area excludes GRBs that cannot be observed by a bolometric detector of threshold $P_{\rm min} = 10^{-7}$ erg cm^{-2} s^{-1}. The thick line corresponds to $E_{\rm p} = 70$ keV. Above this line are also plotted lines for $E_{\rm p} = 150$ keV, 400 keV, 1 MeV, and 3 MeV. Below $E_{\rm p} = 40$ keV and 10 keV are found. The location of GRB980425 is shown as a big dot.

kinetic energy. The afterglow lightcurve in the V band is always well below the lightcurve of SN 1998bw, while it is very close to the *Beppo-SAX* detections or upper limits in X-rays.

4.4. Rate of GRB 980425-like events

The parameters of the internal shock scenario should be given by models of the central engine. However, the production of the relativistic outflow is far from being understood. Therefore, the probability density of parameters, such as the injected kinetic energy flux $\dot{E}$, the mean Lorentz Γ, the constrast κ, and the duration of the relativistic ejection τ are unknown, which prevents us from using the internal shock model to predict the rate of a specific class of GRBs, such as GRB 980425-like events. However, we have shown that in the framework of the internal shock model, "standard" GRBs are produced by highly energetic/highly relativistic outflows, whereas GRB 980425-like events are produced by mildly energetic/mildly relativistic outflows.

That GRB 980425 has been observed (and maybe a somehow similar event with GRB 060218), whereas no "standard" GRB has been observed within a few hundred Mpc, would then indicate that less spectacular relativistic ejections are more probable than the extreme outflows that are needed to produce a "standard" GRB. Indeed, the fraction of stellar collapses that produce bright GRBs is estimated to be of the order of 10^{-6} (apparent rate) (Porciani & Madau 2001), i.e. $\sim 10^{-4}$–10^{-3} after correction for the beaming angle (Frail et al. 2001). Recently Soderberg et al. (2006b) have estimated that the rate of "subenergetic GRBs" (GRB980425-like events) has to be $\sim$10 times higher than the rate of "standard" bright GRBs, which is still compatible with only a fraction of type Ic supernovae being associated with such GRBs if the beaming angle is not too small.

4.5. Non electromagnetic emission

As the rate of GRB 980425-like events is expected to be higher than the rate of "standard" GRBs, it is interesting to investigate whether such weak bursts could contribute in a significant way to the production of non electromagnetic radiation, i.e. ultra-high energy cosmic rays (UHECRs), high energy neutrinos, and gravitational waves. Due to a lower Lorentz factor and a lower kinetic energy, the formalism developed by Waxman (2001) can be used to show that GRB 980425-like events are probably not able to accelerate protons at energies higher than $\sim 10^{19}$ eV. In addition, the low power of these bursts is not compensated

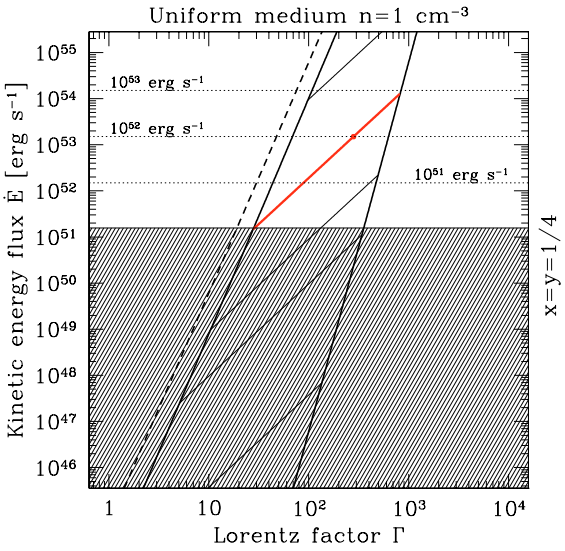

Fig. 5. The internal shock model parameter space at $z = 1$. The diagram plotted in Fig. 4 has been moved from $z = 0.0085$ to $z = 1$, κ, τ, ϵ_e and K being kept constant. Only the case where $x = y = 1/4$ and the external medium has a constant density $n = 1$ cm^{-3} is shown. Weak GRBs are now undetected. The thick line corresponds to $E_p = 150$ keV. Above this line are found $E_p = 400$ keV and 1 MeV. Below are plotted lines for $E_p = 70$ keV, 40 keV and 10 keV. The big dot indicates the location of a "standard" GRB with $E_p = 150$ keV (observer frame) and $L_{rad,4\pi} = 10^{52}$ erg s^{-1}.

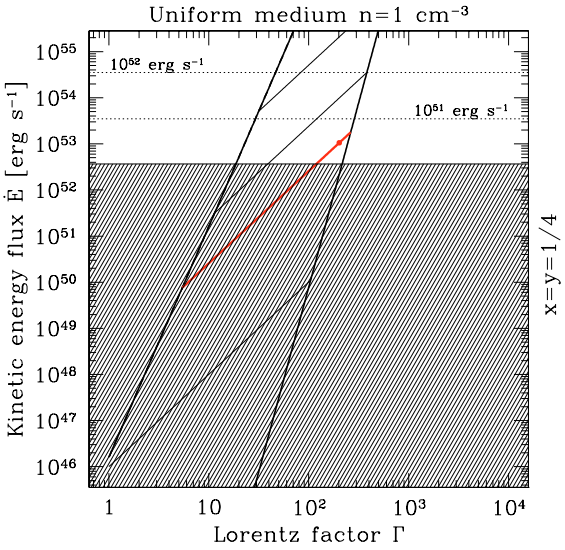

Fig. 6. Effect of the contrast κ. The diagram at $z = 1$ plotted in Fig. 5 has been moved to the situation where the amplitude of the initial variations of the Lorentz factor is low: $\kappa = 1.5$ instead of $\kappa = 4$. All other parameters are the same as in Fig. 5. The thick line corresponds to $E_p = 40$ keV. Both $E_p = 70$ keV and 150 keV are found above this line, while the line $E_p = 10$ keV is plotted below it. The big dot indicates the location of a "standard" XRR with $E_p = 40$ keV (observer frame) and $L_{rad,\,4\pi} = 3 \times 10^{50}$ erg s^{-1}.

by the larger event rate so that the local energy injection rate in UHECRs due to GRB 980425-like events is probably only a few percent of the rate due to "standard GRBs". We conclude that GRB 980425-like events are not good candidates as sources for UHECRs, and they probably do not even contribute significantly to the observed CR spectrum below 10^{19} eV. The same kind of conclusion is reached for high-energy neutrinos.

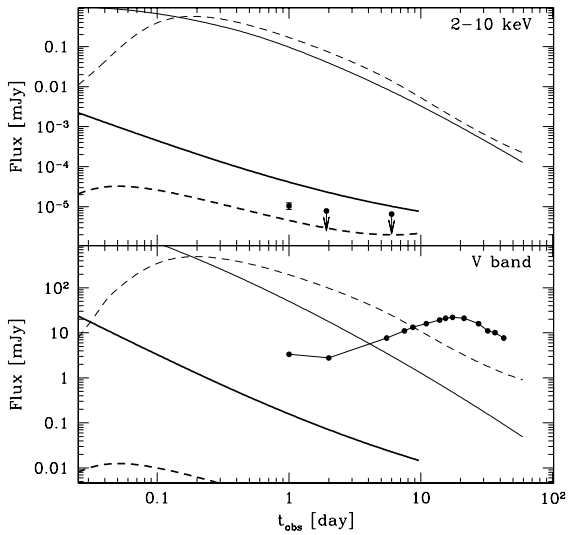

Fig. 7. Afterglow lightcurve in X-rays (*top panel*) and *V* band (*bottom*). The thick lines show the predicted afterglow lightcurve in the case of an intrinsically weak GRB seen on-axis and the thin lines in the case of a bright GRB seen off-axis. The solid lines correspond to a stellar wind environment and the dashed lines to a uniform medium (see text). Observations are shown with filled circles.

Gamma-ray photons of ~100 keV will interact with protons at the photo-meson threshold of the Δ resonance (see e.g. Waxman 2001), i.e. of energy $\sim 2 \times 10^{14}$ eV in the observer frame for $\Gamma = 10$. Due to the decay of the produced pions, neutrinos are emitted, that carry typically 5% of the initial proton energy, i.e. $\sim 10^{13}$ eV. However, the neutrino flux should a priori scale with the high-energy proton flux, and therefore the contribution of GRB 980425-like events should be only a small fraction of the total GRB contribution.

The prospects are much better for gravitational waves. Long GRBs are believed to be associated with massive stars that collapse into black holes (Woosley 1993). As only a fraction of these collapses lead to the production of a gamma-ray burst, peculiar conditions are required. It is natural to expect that a high rotation of the progenitor favors GRBs, as the ultra-relativistic outflow is probably easier to eject along the rotation axis. Therefore, collapsars might be asymmetric and then produce gravitational waves. This is also supported by the physical modelling of SN1998bw, which probably requires a high degree of asymmetry (Höflich et al. 1999; Nakamura et al. 2001). Kobayashi & Mészáros (2003) estimate the expected signal for an asymmetric stellar collapse to be on the order of $h \sim 10^{-22}$ in the 100–1000 Hz range at ~30 Mpc for plausible parameters. Such a signal will be detected by advanced gravitational waves detectors. It is interesting to note that in the proposed scenario the nature of the initial event responsible for GRB 980425 may not be any different than for "standard" GRBs. This is supported by the similarities between SN2003dh (associated with GRB 030329 at $z = 0.168$) and SN 1998bw. The emission of gravitational waves of GRB 980425-like events may thus be comparable to those expected for "standard" long GRBs. Due to their higher rate within a few 10 Mpc, GRB 980425-like events are therefore very promising sources for advanced GW detectors (Norris 2003).

5. Conclusion

We have investigated two scenarios to explain GRB 980425-like events:

- in the first scenario, GRB 980425 is a normal (intrinsically bright) GRB seen off-axis. A viewing angle that is greater than the opening angle of the jet by a few $1/\Gamma$ is enough to produce an apparently weak GRB like 980425. However, this scenario suffers several problems: (1) the afterglow of GRB 980425 should have been very bright and therefore detected, and (2) the rate of GRB 980425-like events should be very low. If we exclude the possibility that we have observed an extremely rare event by chance and if we take into account that a local on-axis intrinsically bright GRB has never been observed, we get two strong constraints: the local rate of "standard" bright GRBs has to be much higher than what can be simply extrapolated from the cosmic event rate and, at the same time, the typical jet opening angle in GRBs must be much narrower than what is usually inferred from observations of breaks in afterglow lightcurves.
- *Since this contradicts our current understanding of the GRB physics, we prefer the second scenario, where GRB 980425 is an intrinsically low-luminosity GRB seen on-axis.* We have shown that the parameter space of the internal shock model allows such events, which would be produced by mildly relativistic ($\Gamma \sim 10-20$), mildly energetic ($\dot{E} \simeq 5 \times 10^{47}$ erg s^{-s}) outflows. The consequences are that (1) in collapsars, the central engine in most cases fails to power a highly-relativistic/highly-energetic ejection (necessary for bright "standard" GRBs) but can more easily power a mildly relativistic/mildly energetic outflow. The fraction of collapsars that succeed in producing a highly-relativistic/energetic or a mildly relativistic/energetic outflow is, of course, not necessarily constant in time. There is indeed increasing evidence in favor of an evolution, indicating that relativistic ejection is easier at low metallicity (see e.g. Le Floc'h et al. 2006; Daigne et al. 2006; Stanek et al. 2006). (2) The rate of GRB 980425-like intrinsically weak events in the Universe is then much higher than the rate of "standard" intrinsically bright GRBs, but the apparent rate is lower because these events can be detected only at low redshift. Finally, as this scenario infers a higher local rate for GRB 980425-like events compared to "standard" bright GRBs, we have discussed the possible non-electromagnetic emission of these bursts. We find that they are not promising sources of UHECRs and high-energy neutrinos, as the corresponding flux probably scales with the gamma-ray flux. On the other hand, since GRB 980425 was associated with an extreme type Ic supernova such as those associated with "standard" long GRBs, one can expect the corresponding stellar collapse to be asymmetric, and GRB 980425-like events could therefore be promising sources of gravitational waves within a few 10 Mpc.

References

Band, D. L. 2003, ApJ, 588, 945
Band, D., Matteson, J., Ford, L., et al. 1993, ApJ, 413, 281
Baring, M. G. 1995, Ap&SS, 231, 169
Barraud, C., Olive, J.-F., Lestrade, J. P., et al. 2003, A&A, 400, 1021
Barraud, C., Daigne, F., Mochkovitch, R., & Atteia, J. L. 2005, A&A, 440, 809
Bosnjak, Z., Celotti, A., Ghirlanda, G., Della Valle, M., & Pian, E. 2006, A&A, 447, 121
Cusumano, G., Barthelmy, S., Gehrels, N., et al. 2006, GRB Coordinates Network, 4755
Daigne, F., & Mochkovitch, R. 1998, MNRAS, 296, 275
Daigne, F., & Mochkovitch, R. 1999, A&AS, 138, 523
Daigne, F., & Mochkovitch, R. 2000, A&A, 358, 1157
Daigne, F., & Mochkovitch, R. 2001, in Gamma-ray Bursts in the Afterglow Era, ed. E. Costa, F. Frontera, & J. Hjorth, 324
Daigne, F., & Mochkovitch, R. 2002, MNRAS, 336, 1271
Daigne, F., & Mochkovitch, R. 2003, MNRAS, 342, 587
Daigne, F., & Mochkovitch, R. 2004, in Gamma-Ray Bursts: 30 Years of Discovery, ed. E. Fenimore, & M. Galassi, AIP Conf. Proc., 727, 328
Daigne, F., Rossi, E. M., & Mochkovitch, R. 2006, MNRAS, 372, 1034
Frail, D. A., Kulkarni, S. R., Sari, R., et al. 2001, ApJ, 562, L55
Frontera, F., Amati, L., Costa, E., et al. 2000, ApJS, 127, 59
Galama, T. J., Vreeswijk, P. M., van Paradijs, J., et al. 1998, Nature, 395, 670
Ghisellini, G., Ghirlanda, G., Mereghetti, S., et al. 2006, MNRAS, 372, 1699
Golenetskii, S. V., Mazets, E. P., Aptekar, R. L., & Ilinskii, V. N. 1983, Nature, 306, 451
Granot, J., Piran, T., & Sari, R. 1999, ApJ, 513, 679
Guetta, D., Perna, R., Stella, L., & Vietri, M. 2004, ApJ, 615, L73
Heise, J., in't Zand, J., Kippen, R. M., & Woods, P. M. 2001, in Gamma-ray Bursts in the Afterglow Era, ed. E. Costa, F. Frontera, & J. Hjorth, 16
Höflich, P., Wheeler, J. C., & Wang, L. 1999, ApJ, 521, 179
Kippen, R. M., Woods, P. M., Heise, J., et al. 2001, in Gamma-ray Bursts in the Afterglow Era, ed. E. Costa, F. Frontera, & J. Hjorth, 22
Kobayashi, S., & Mészáros, P. 2003, ApJ, 589, 861
Kouveliotou, C., Woosley, S. E., Patel, S. K., et al. 2004, ApJ, 608, 872
Le Floc'h, E., Charmandaris, V., Forrest, W. J., et al. 2006, ApJ, 642, 636
Liang, E., & Kargatis, V. 1996, Nature, 381, 49
Lithwick, Y., & Sari, R. 2001, ApJ, 555, 540
Masetti, N., Palazzi, E., Pian, E., Patat, F., et al. 2006, GRB Coordinates Network, 4803
Meszaros, P., & Rees, M. J. 1997, ApJ, 476, 232
Mészáros, P., & Rees, M. J. 2000, ApJ, 530, 292
Mirabal, N., Halpern, J. P., An, D., Thorstensen, J. R., & Terndrup, D. M. 2006, ApJ, 643, L99
Nakamura, T. 1999, ApJ, 522, L101
Nakamura, T., Mazzali, P. A., Nomoto, K., & Iwamoto, K. 2001, ApJ, 550, 991
Norris, J. P. 2003, in The Astrophysics of Gravitational Wave Sources, ed. J. M. Centrella, AIP Conf. Proc., 686, 74
Norris, J. P., Marani, G. F., & Bonnell, J. T. 2000, ApJ, 534, 248
Perna, R., Sari, R., & Frail, D. 2003, ApJ, 594, 379
Pian, E., Amati, L., Antonelli, L. A., et al. 2000, ApJ, 536, 778
Porciani, C., & Madau, P. 2001, ApJ, 548, 522
Preece, R. D., Briggs, M. S., Mallozzi, R. S., et al. 2000, ApJS, 126, 19
Rees, M. J., & Meszaros, P. 1994, ApJ, 430, L93
Rossi, E., Lazzati, D., & Rees, M. J. 2002, MNRAS, 332, 945
Salmonson, J. D. 2001, ApJ, 546, L29
Sazonov, S. Y., Lutovinov, A. A., & Sunyaev, R. A. 2004, Nature, 430, 646
Schmidt, M. 2001, ApJ, 552, 36
Soderberg, A. M., Kulkarni, S. R., Berger, E., et al. 2004, Nature, 430, 648
Soderberg, A., Berger, E., & Schmidt, B. 2006a, IAU Circ., 8674, 2
Soderberg, A. M., Kulkarni, S. R., Nakar, E., et al. 2006b, Nature, 442, 1014
Stanek, K. Z., Gnedin, O. Y., Beacom, J. F., et al. 2006, Acta Astron., 56, 333
Stanek, K. Z., Matheson, T., Garnavich, P. M., et al. 2003, ApJ, 591, L17
Waxman, E. 2001, LNP: Physics and Astrophysics of Ultra-High-Energy Cosmic Rays, 576, 122
Waxman, E. 2004a, ApJ, 605, L97
Waxman, E. 2004b, ApJ, 602, 886
Woods, E., & Loeb, A. 1999, ApJ, 523, 187
Woosley, S. E. 1993, ApJ, 405, 273
Yamazaki, R., Yonetoku, D., & Nakamura, T. 2003, ApJ, 594, L79